

Article

Estimation of Runoff and Sediment Yield in Response to Temporal Land Cover Change in Kentucky, USA

Smriti Kandel¹, Buddhi Gyawali^{2,*}, Sandesh Shrestha², Demetrio Zourarakis³, George Antonious², Maheteme Gebremedhin² and Bijay Pokhrel⁴

¹ College of Engineering, The University of Texas at Arlington, Arlington, TX 76019, USA

² College of Agriculture, Community, and the Sciences, Cooperative Extension Building, Kentucky State University, Frankfort, KY 40601, USA

³ Department of Plant and Soil Sciences, University of Kentucky, Lexington, KY 40506, USA

⁴ Builder First Source, Dallas, TX 75201, USA

* Correspondence: buddhi.gyawali@kysu.edu

Abstract: Land cover change is prevalent in the eastern Kentucky Appalachian region, mainly due to increased surface mining activities. This study explored the potential change in land cover and its relationship with stream discharge and sediment yield in a watershed of the Cumberland River near Harlan, Kentucky, between 2001 and 2016, using the Soil and Water Assessment Tool (SWAT). Two land cover scenarios for the years 2001 and 2016 were used separately to simulate the surface runoff and sediment yield at the outlet of the Cumberland River near Harlan. Land cover datasets from the National Land Cover Database (NLCD) were used to reclassify the land cover type into the following classes: water, developed, forest, barren, shrubland, and pasture/grassland. Evaluation of the relationship between the land cover change on discharge and sediment was performed by comparing the average annual basin values of streamflow and sediment from each of the land cover scenarios. The SWAT model output was evaluated based on several statistical parameters, including the Nash–Sutcliffe efficiency coefficient (NSE), RMSE-observations standard deviation ratio (RSR), percent bias (PBIAS), and the coefficient of determination (R^2). Moreover, P-factor and R-factor indices were used to measure prediction uncertainty. The model showed an acceptable range of agreement for both calibration and validation between observed and simulated values. The temporal land cover change showed a decrease in forest area by 2.42% and an increase in developed, barren, shrubland, and grassland by 0.11%, 0.34%, 0.53%, and 1.44%, respectively. The discharge increased from 92.34 mm/year to 104.7 mm/year, and sediment increased from 0.83 t/ha to 1.63 t/ha from 2001 to 2016, respectively. Based on results from the model, this study concluded that the conversion of forest land into other land types could contribute to increased surface runoff and sediment transport detached from the soil along with runoff water. The research provides a robust approach to evaluating the effect of temporal land cover change on Appalachian streams and rivers. Such information can be useful for designing land management practices to conserve water and control soil erosion in the Appalachian region of eastern Kentucky.

Keywords: eastern Kentucky; land cover; sediment; surface runoff; SWAT; watershed



Citation: Kandel, S.; Gyawali, B.; Shrestha, S.; Zourarakis, D.; Antonious, G.; Gebremedhin, M.; Pokhrel, B. Estimation of Runoff and Sediment Yield in Response to Temporal Land Cover Change in Kentucky, USA. *Land* **2023**, *12*, 147. <https://doi.org/10.3390/land12010147>

Academic Editor: Manuel López-Vicente

Received: 14 August 2022

Revised: 10 December 2022

Accepted: 13 December 2022

Published: 1 January 2023



Copyright: © 2023 by the authors. Licensee MDPI, Basel, Switzerland. This article is an open access article distributed under the terms and conditions of the Creative Commons Attribution (CC BY) license (<https://creativecommons.org/licenses/by/4.0/>).

1. Introduction

The term “watershed” refers to an area of land that channels precipitation to water reservoirs such as creeks, streams, bays, and the ocean [1]. The term “land cover” indicates the physical land type, such as forest, water, cropland, wetland, etc., whereas land use represents how people are using the land [2]. Human activities cause changes in land cover patterns, resulting in alteration of the hydrological components of the watershed, such as runoff, infiltration, evapotranspiration, and hence, a change in annual mean discharge [3–5]. Non-Point Source (NPS) pollution, which is primarily the runoff of contaminants from

mining operations due to excess rainfall, is a major concern in the Appalachian Region that pollutes streams, lakes, and creeks. Pollutants such as chemicals (nitrates, phosphates), trace elements, heavy metals, and pathogens may be transported both in solution and in the attached form with sediment, defined as suspended soil particles. These major pollutants affect surface water quality as well as damage the aesthetic values of waterbodies.

Temporal land cover change is one of the most important factors that affect surface water characteristics [6]. Land cover change can lead to changes in flow patterns due to spatial variations in runoff formation due to climate–land use interaction and can alter other related hydrologic processes such as evapotranspiration, runoff, sediment, and nutrient transport to water [7–10]. It is important to assess the effect of land cover changes for environmental assessment, land management, and its impacts on human well-being in the human–environment interaction [11,12].

Some types of land cover change are intensive, such as surface mining, which extracts minerals (e.g., coal) from the seams near the Earth's surface [13]. The primary types of mining include underground, contour, and mountaintop removal or surface coal mining in the Appalachia Region. Mountain top removal mining is the most common form of surface coal mining in the region. The use of modern techniques, such as heavy equipment, during mining, can produce dramatic ecological and hydrological alterations in land cover [14]. Surface coal mining, which directly strips away the vegetation of the mined areas, involves a sequence of operations, including clearing vegetation, removing topsoil, drilling, and blasting hard surface strata over the coal layer, then subsequently extracting and transporting coal [15]. The specific impacts of mountaintop removal mining generally observed in Central Appalachia are loss of natural forests, hydrological pattern changes, valley fill, acid drainage, and water quality degradation. Mining activities result in a change of topography and drainage pattern, further causing soil erosion and land degradation [16,17]. Central Appalachia has the highest earth movement rate in the United States, with each surface mine generating large quantities of spoil that are typically translocated to stream valleys close to mining areas [18]. Generally, mined areas are reclaimed after the completion of the mining operation, which is the combined process by which adverse environmental effects of surface mining are minimized. Reclaimed mine lands are more prone to soil erosion, leading to subsequent biomass loss even after reclamation [19,20]. Reclamation efforts are expected to control erosion and sedimentation, stabilize slopes, and repair wildlife habitat [21]. However, mine reclamation leaves the land barren or converts the originally forested area into grassland and shrublands. Therefore, even after reclamation, the geological changes and associated environmental impacts may continue if mine lands are not appropriately backfilled [22].

The Appalachian region of the eastern part of Kentucky (in the US), covering 31 counties with a combined land area of 34,628 km², is known for coal [23]. A study of land cover change in Kentucky reported that forest areas were transformed into barren land and grasslands cumulatively in mined areas due to mining and reclamation activities [24]. These authors also reported that mining and reclamation are major drivers of overall land cover change in eastern Kentucky. Another study in Kentucky showed that land cover change has a greater impact on soil loss and retention, contributing to an increase in total nitrogen and phosphorus export between 1992 and 2011 [25].

According to the Kentucky Division of Water [26], NPS pollution is a major contributor to contamination in Kentucky's waterways. Among the non-point source, primary pollutants are mining (31%), agriculture (29%), land disposal (20%), and urban runoff (10%) [27]. Surface-coal mine areas disturb natural infiltration and surface flow of headwater streams, causing land degradation and impacting hydrologic characteristics [28–30]. Physical degradation happens when excess debris is placed in valleys, resulting in the burial or loss of stream channels. Water quality and aquatic habitats are impaired when dissolved elements, major ions, and heavy metals are released from mine debris and transported into stream waters [31].

The Soil and Water Assessment Tool (SWAT) is one of the most widely adopted watershed models worldwide used to predict surface runoff and sediment yields over a long period in complex catchments with different soils and land use [32]. The SWAT model has been widely used to simulate changes in hydrology and water quality (nutrients and sediment) in watersheds under different climatic conditions, land use practices, and land cover changes [33–37]. Taking the hydrological behavior of the watershed into consideration, the application of the SWAT model integrated with GIS and remote sensing can be used to estimate surface runoff and sediment yield. Various studies have been conducted worldwide to understand the relationship between land cover change and hydrological processes in watersheds at different spatial and temporal scales by using the SWAT model. For example, Zhang et al. [35] used the SWAT model to simulate runoff and sediment yield responses to land use change in China and found that forestland decreased sediment yield and reduced runoff. However, they reported increased runoff and sediment yield in cropland and urban land. Similarly, Pokhrel [33] analyzed the impact of land use changes on river discharge and sediment yield from 2000 to 2010 at the Khokana gauging station of Kathmandu valley, Nepal. Findings showed an increase in built-up areas, resulting in an increase in the surface runoff and sediment yield. Aboelnour et al. [38] studied land use change impact on streamflow and baseflow in the Little Eagle Creek watershed in Indianapolis, USA. The study found a 39% increase in urbanization, which significantly influenced base flow and streamflow. Spruill et al. [39] used the SWAT model to simulate daily streamflow in a small central Kentucky watershed over a two-year period. Likewise, Yonaba et al. [10] used SWAT to show that dynamic land use conditions affect surface runoff and hydrological processes in the Sahelian landscape.

Several mining operations are prevalent in eastern Kentucky, causing land cover changes that result in a decrease in forested land and an increase in its impact on watersheds. It is necessary to document the land cover of the watershed region and its relationship with the surface runoff and sediment. Although SWAT is the most popular model worldwide for simulating runoff and sediment yield, its application is very limited in Kentucky (SWAT Literature Database https://www.card.iastate.edu/swat_articles/add.aspx (accessed on 14 January 2020)) [40,41]. To fill this research gap, our study applied the SWAT model to explore the watershed characteristics, hydrology, and sediment in the Appalachian region of eastern Kentucky. There is a need to study the hydrologic attributes in response to the land cover change in Kentucky. The research undertaken on a watershed of the Cumberland River near Harlan, Kentucky, with an area of 969 km², had the following objectives: (1) to assess the land cover change between the years 2001 and 2016; (2) to estimate discharge changes due to temporal change in land cover; and (3) to estimate sediment loads as a response to changes in land cover.

2. Materials and Methods

2.1. Study Site

The outlet of the Cumberland River near Harlan, Kentucky, is located at the point where the monitoring station (USGS 05130101) is installed. The site lies at Latitude 36°50'48" and Longitude 83°21'21". The elevation of this watershed varies from 348 m to 1259 m. The watershed has a drainage area of 969 km². The observed daily discharge and sediment data record for this site is maintained by the USGS National Water Information System.

Figure 1 shows the geographic location of the study area, a watershed of the Cumberland River near Harlan, which lies in Harlan County but also shares a part of Letcher County. Harlan County is in southeastern Kentucky, sharing the border with Bell County, Kentucky; Leslie County, Kentucky; Letcher County, Kentucky; Perry County, Kentucky; Lee County, Virginia; and Wise County, Virginia. The county has a total area of 1212 km², out of which 1207 km² is land, and the remaining is water. The highest elevation point of Kentucky, Black Mountain (1263 m), is located in Harlan County. The total population of Harlan County was 29,278 in 2020, out of which 31.1% of residents live in poverty [42]. The

weather data were obtained from Prism Climate Group (<https://prism.oregonstate.edu/> (accessed on 20 April 2020)). The variation in annual precipitation, maximum temperature, and minimum temperature of Harlan County between the years 1990 and 2019 are shown below in Figure 2. This study site was selected due to the availability of observed discharge and sediment data at the outlet point.

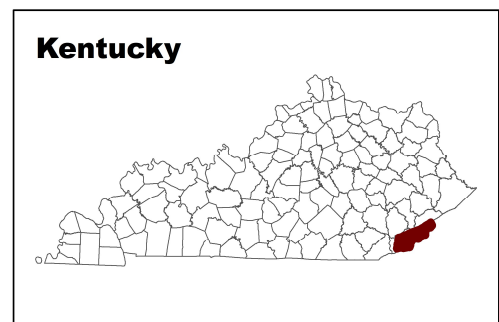
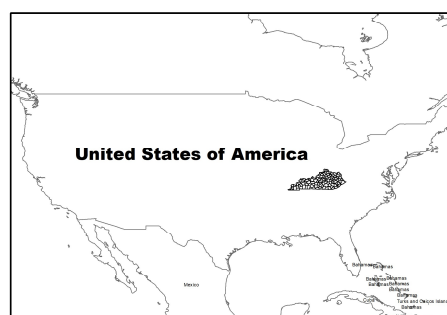
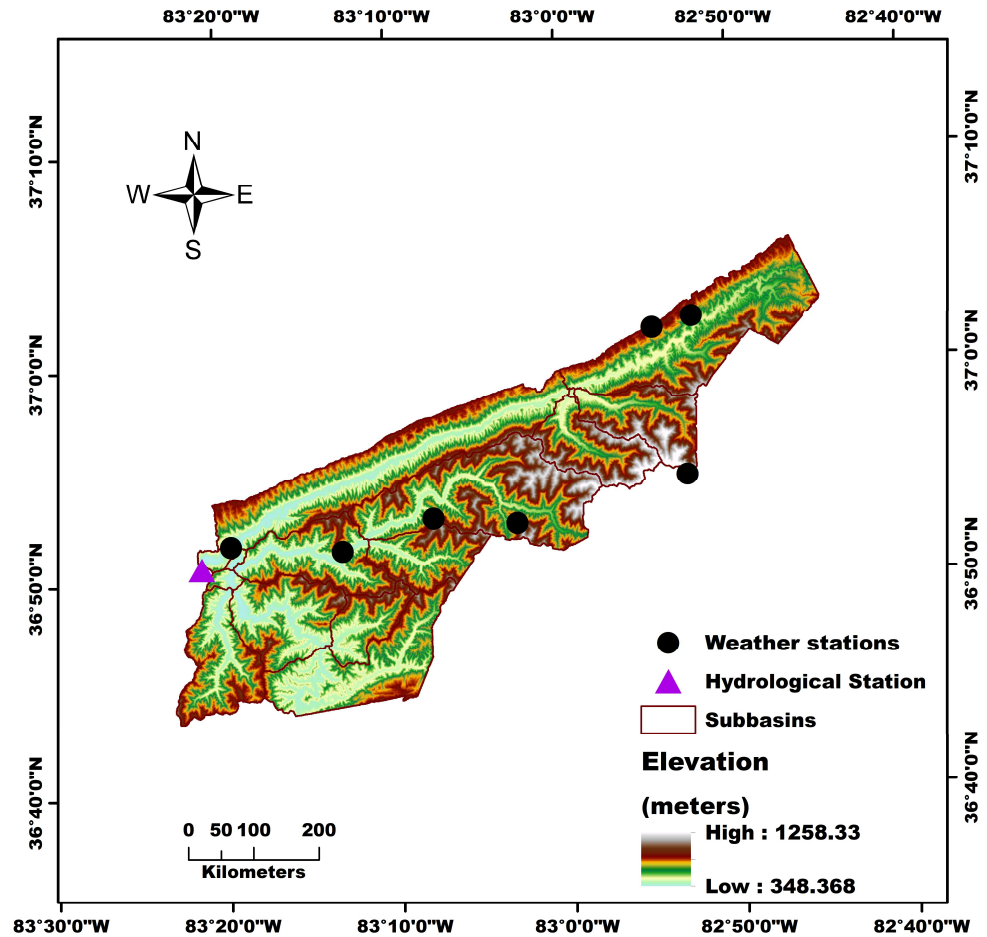


Figure 1. Location of the study area (watershed of the Cumberland River near Harlan, Kentucky).

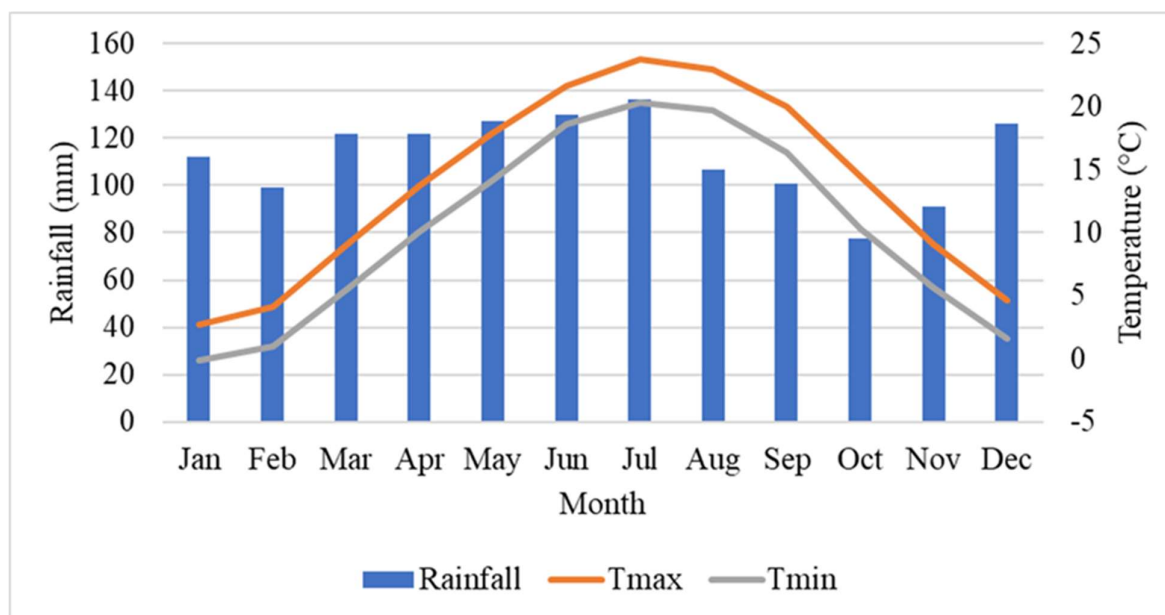


Figure 2. Average monthly rainfall, maximum and minimum temperature at Harlan County, Kentucky (1990–2019). Data Source: PRISM Climate Group (<https://prism.oregonstate.edu/normals/> (accessed on 20 April 2020)).

2.2. SWAT Model

This study used the SWAT model to simulate surface runoff and sediment for the watershed in our study. SWAT is a continuous-time, semi-distributed, and process-based river basin model, which was developed to predict the effect of alternative land management practices on water, sediment, and chemicals from ungauged rural basins in large complex watersheds [43,44]. SWAT model has been widely used and proven to be effective in studying the impacts of climate and land use on water quantity and quality [45,46].

The model is supported by online documentation [47] and geographic information systems (GIS) interface tools. The model is process-based, computationally efficient, and capable of continuous simulation over a longer period. This model requires input information about weather, such as daily precipitation, maximum/minimum temperature, solar radiation, wind speed, relative humidity, soil, topography, and land cover. For modeling purposes, a watershed is divided into a number of sub-watersheds or sub-basins. Sub-watersheds are further divided into hydrologic response units (HRUs). Each HRU consists of homogeneous land cover, management, topographic characteristics, and soil type. Runoff is predicted separately for each HRU by using daily or sub-daily rainfall amounts that are then routed to obtain the total runoff for the watershed, which increases accuracy and creates a better physical description of the water balance [41,47]. SWAT uses the Modified Universal Soil Loss Equation (MUSLE) to predict sediment yield from the landscape [48].

2.3. SWAT Input Data

The data required for this study were collected from various sources, as shown in Table 1. ArcMap version 10.7 (Esri geospatial software) was used to prepare DEM and soil maps. The SSURGO soil classes and slope classes for the study area are shown in Figure 3 and in the Appendix A.

Table 1. Input data for SWAT model.

Data	Measurable Unit	Spatial Unit	Year	Source
Digital Elevation Model (DEM)	Pixel level	30 m × 30 m resolution	2020	https://kygeoportal.ky.gov/ (accessed on 12 April 2020). USDA (SSURGO)
Soil (Physical properties)	Shapefile		2020	www.nrcs.usda.gov (accessed on 12 April 2020)
Land cover	Pixel level	30 m × 30 m resolution	2001 and 2016	Multi-Resolution Land Cover Characteristics (MRLC) Consortium, https://www.mrlc.gov/ (accessed on 12 April 2020)
Meteorological (rainfall, solar radiation, temperature, humidity, wind velocity)	Table, txt	Daily data	1987–2016	Prism Climate Group https://prism.oregonstate.edu/ (accessed on 20 April 2020), Global weather Data for SWAT https://globalweather.tamu.edu/
Discharge	Monthly (m ³ /s)		1990–2005	https://waterdata.usgs.gov/nwis (accessed on 15 April 2020)
Sediment	Monthly (ton/ha)		1990–2005	https://waterdata.usgs.gov/nwis (accessed on 15 April 2020), LOADEST

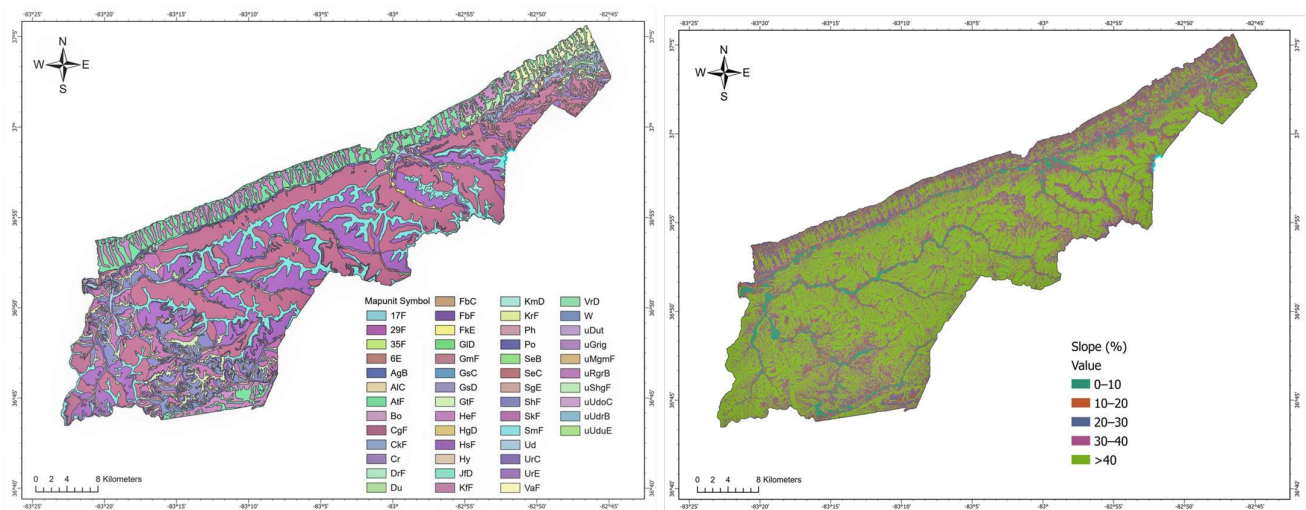


Figure 3. Input data for the SWAT model: a. Soil classes and b. Slope map of the Cumberland River near Harlan watershed.

Land cover data for both years 2001 and 2016 (Figure 4a,b) were extracted for the study area and reclassified into six land cover types: water, urban, barren, forest, shrubland, and pasture/grassland. Additionally, to check the quality and validity of input land cover data in SWAT, an accuracy assessment was performed using the Image Analyst Tool in ArcGIS Pro. The accuracy assessment points (500 points) were generated randomly, and the ground truth classes for these points were identified by using a reference land cover map for respective years, i.e., years 2001 and 2016. The confusion matrix method was used to assess the accuracies of land cover classes. We derived the Kappa value of 0.84, which is 84% accuracy of our reclassified land cover data.

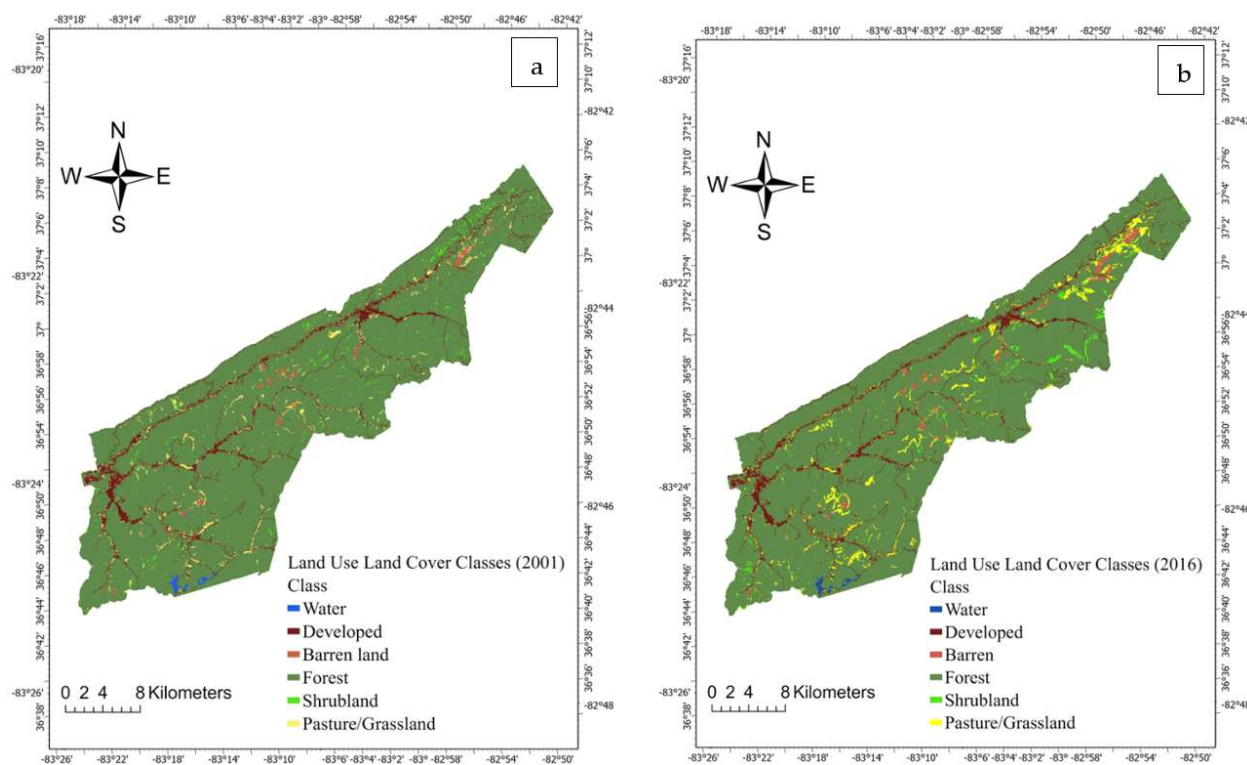


Figure 4. Land use and land cover map of the study area for the years 2001 (a) and 2016 (b).

The daily precipitation, maximum temperature, and minimum temperature information were obtained from Prism Climate Group (PRISM) (<https://prism.oregonstate.edu/> (accessed on 20 April 2020)) for seven different stations to set up the model. Wind speed, solar radiation, and relative humidity were simulated using the weather generator in SWAT. Discharge and sediment data at the outlet of Cumberland River near Harlan were obtained from USGS National Water Information System (NWIS) (<https://waterdata.usgs.gov/nwis> (accessed on 15 April 2020)). The sediment data were available from NWIS only from 1979 to 1981, which was used to simulate the calibration and validation period using a load estimator (LOADEST). LOADEST is a program for estimating constituent loads in streams and rivers [49]. We used LOADEST to extrapolate scarce nutrient/sediment data corresponding to stream flow. Generally, we have relatively few nutrient/sediment concentration data that do not cover the whole simulation period. Several peer-review papers and reports have used LOADEST for extrapolating nutrient/sediment data to the simulation period. Nine predefined models vary with the number of explanatory variables available in the LOADEST framework. The selection of the best model is based on the lowest value for Akaike Information Criterion (AIC), the highest value of the Schwarz Posterior Probability Criterion (SPPC), Load Bias Percent (Bp) less than 25%, higher Nash–Sutcliffe Efficiency (NSE), and higher coefficient of determination (R^2) values. We have selected model 6, which satisfies the above criteria.

2.4. SWAT Model Setup

ArcSWAT 2012, a GIS interface, was used to delineate the watershed at the outlet point of the Cumberland River near Harlan, Kentucky. Figure 5 shows a flow chart of surface runoff and sediment yield simulation using the SWAT model. This study used a 10% threshold set for land cover, soil type, and slope, which resulted in 15 sub-basins and 168 HRUs. The model was run for three years (1987–1989) of the warm-up period on a monthly basis.

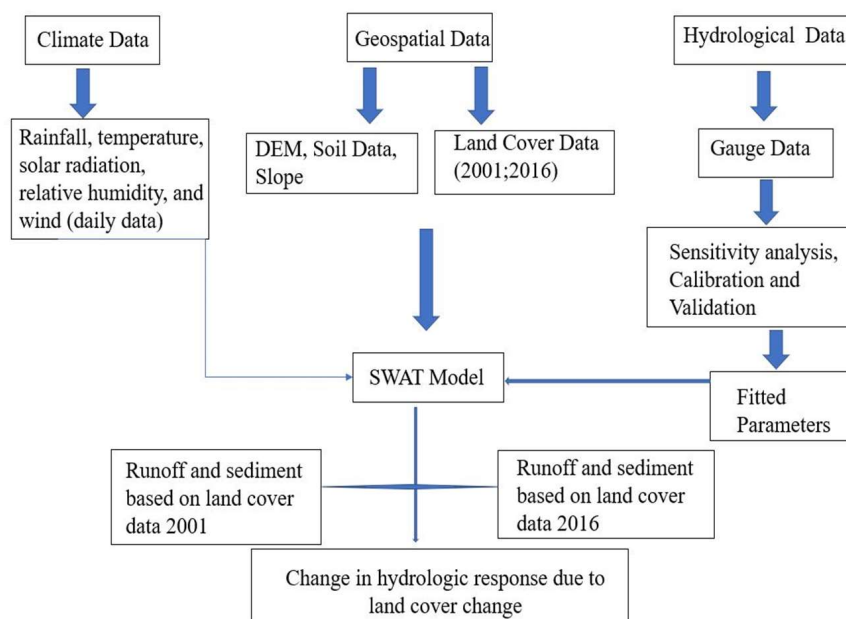


Figure 5. Workflow for SWAT model.

2.5. Sensitivity Analysis

This study used SWAT-CUP Premium (SWAT-CUPP), a computer program developed for calibration of the SWAT model (<https://www.2w2e.com/home/SwatCupPremium> (accessed on 23 October 2020)). SWAT-CUPP is an improved version of SWAT-CUP, which allows behavioral and multi-objective calibration. The program also allows validation, sensitivity analysis, and uncertainty analysis [50]. Users can select several choices of objective functions (11 functions, including Nash–Sutcliffe Efficiency coefficient [NSE], the coefficient of determination [R^2], and percent bias (PBIAS)). In this study, we selected NSE as our objective function for reflecting the overall fit of a hydrograph [51–53].

Sensitivity analysis is an essential part of a model setup. It helps in determining the most significant and sensitive parameters altering the water quantity and quality yields. Sensitivity analysis is the process of determining the rate of change in model output with respect to change in model inputs. It is necessary to decide on key parameters required for calibration. This study used global sensitivity analysis to rank the model parameters and to account for the interaction between various parameters.

Global sensitivity analysis uses a multiple regression system that regresses the Latin hypercube-generated parameters against objective function values to determine the sensitive parameters. Statistical measurements, including t-statistics and p-values at 0.05 level of significance, are used to identify the sensitive parameters. The parameters with larger t-statistics and smaller p-value were considered significantly sensitive parameters. The most frequently used parameters reported in multiple prior studies were used for sensitivity analysis, calibrating, and validating the SWAT model for discharge and sediment [33,54]. The calibrated parameters, their definition, and the initial range of values are presented in Table 2. Eighteen different parameters were used with one iteration (600 simulations each) to perform global sensitivity analysis for discharge. Once satisfactory calibration performance was obtained for discharge, sensitivity analysis was carried out for the sediment parameters with a similar approach as discharge. The initial ranges for the selected parameters were used from the absolute value range provided by SWAT-CUPP, recommended in the SWAT-CUP user manual [55,56].

Table 2. Parameters used to calibrate discharge and sediment yield (v = replace, r = relative).

Parameters	Definition	Unit	Default Range of Values	Values Set in SWAT-CUPP
Parameters for Discharge				
r_CN2.mgt	SCS runoff curve number for moisture condition II	-	35 to 98	−0.4 to 0.5
r_SOL_K().sol	Saturated hydraulic conductivity	mm/hr	0 to 2000	−0.5 to 0.5
r_SOL_AWC().sol	Available water capacity of the soil layer	mm H ₂ O/mm soil	0 to 1	−0.5 to 0.5
r_SOL_BD().sol	Moist bulk density	Mg/m ³ or g/cm ³	0.9 to 2.5	−0.5 to 0.5
v_CH_K2.rte	Effective hydraulic conductivity in main channel alluvium	mm/hr	−0.01 to 500	−0.01 to 500
r_HRU_SLP.hru	Average slope steepness	m/m	0 to 0.6	−0.5 to 0.5
v_RCHRG_DP.gw	Deep aquifer percolation fraction	-	0 to 1	0 to 1
v_GWQMN.gw	Threshold depth of water in the shallow aquifer required for return flow to occur	mm H ₂ O	0 to 5000	0 to 5000
v_ESCO.hru	Soil evaporation compensation factor	-	0 to 1	−0.5 to 0.5
r_SLSUBBSN.hru	Average slope length.	m	10 to 150	−0.5 to 0.5
v_GW_DELAY.gw	Groundwater delay	days	0 to 500	0 to 500
v_GW_REVAP.gw	Groundwater “revap” coefficient.	-	0.02 to 0.2	0.02 to 0.2
v_REVAPMN.gw	Threshold depth of water in the shallow aquifer for “revap” to occur (mm).	mm	0 to 1000	0 to 1000
v_ALPHA_BF.gw	Baseflow alpha factor (days)	days	0 to 1	0 to 1
r_OV_N.hru	Manning’s “n” value for overland flow	-	0.01 to 4	−0.5 to 0.5
v_SURLAG.bsn	Surface runoff lag time	-	0.05 to 24	0.05 to 24
v_CH_N2.rte	Manning’s “n” value for the main channel	-	−0.01 to 0.3	−0.01 to 0.3
Parameters for sediment				
v_PRF.bsn	Peak rate adjustment factor for sediment routing in the main channel	-	0 to 2	0 to 2
v_SPCON.bsn	Linear parameter for calculating the maximum amount of sediment that can be re-entrained during channel sediment routing	-	0.0001 to 0.01	0.0001 to 0.01
v_SPEXP.bsn	Exponent parameter for calculating sediment re-entrained in channel sediment routing	-	1 to 1.5	1 to 1.5
v_CH_COV1.rte	Channel erodibility factor	-	−0.001 to 1	−0.05 to 0.6
v_USLE_K.sol	USLE equation soil erodibility (K) factor	(metric ton m ² hr)/(m ³ -metric ton cm)	0 to 0.65	0 to 0.65

Table 3 shows parameters, their fitted values, and their ranking according to sensitivity for discharge. Among the calibrated parameters, v_ALPHA_BF.gw, r_CN2.mgt, and r_SOL_BD ().sol were the most sensitive, followed by r_SOL_K ().sol, v_RCHRG_DP.gw, r_HRU_SLP.hru, whereas v_GW_DELAY.gw and r_SLSUBBSN.hru were fewer sensitive parameters at our watershed.

Table 3. Parameters with their fitted values and ranking according to sensitivity (v = replace, r = relative).

Parameters	Fitted Value	p-Value	t-Stat	Ranking
v_ALPHA_BF.gw	0.57	0.0	15.22	1
r_CN2.mgt	0.39	0.0	9.57	2
r_SOL_BD().sol	0.46	0.0	7.33	3
r_SOL_K().sol	−0.25	0.0000025	4.74	4
v_RCHRG_DP.gw	0.50	0.0000056	4.58	5
r_HRU_SLP.hru	−0.35	0.000086	3.95	6
r_SOL_AWC().sol	−0.40	0.0001	−3.91	7
v_ESCO.hru	0.30	0.00022	3.70	8
v_CH_N2.rte	0.009	0.0018	−3.13	9
v_CH_K2.rte	129.49	0.0039	−2.89	10
v_GWQMN.gw	1695.83	0.005	−2.81	11
r_OV_N.hru	−0.21	0.52	0.62	12
v_REVAPMN.gw	684.16	0.64	−0.46	13
v_SURLAG.bsn	3.66	0.75	−0.31	14
v_GW_REVAP.gw	0.03	0.81	−0.22	15
r_EPCO.hru	0.49	0.83	0.20	16
r_SLSUBBSN.hru	0.16	0.89	−0.13	17
v_GW_DELAY.gw	79.58	0.91	0.11	18

2.6. Model Calibration, Uncertainty Analysis, and Validation

The calibration, uncertainty analysis, and validation of discharge and sediment were completed on a monthly scale at the gauge stations in the watershed under study. Calibration is closely linked to model output uncertainty, which refers to the propagation of all model input uncertainties mapped in the parameter distribution to model outputs [45,46]. SWAT-CUPP uses two indices, P-factor and R-factor, as measures to examine the fit between simulation results expressed as 95PPU, and observation expressed as a single signal, respectively. P-factor is the percentage of observed data enveloped by our modeling result. The 95PPU of its values ranges from 0 to 1, where 1 represents perfect model simulation considering the uncertainty. The R-factor measures the thickness of the 95PPU band. For discharge, P-factor > 0.7 and R-factor < 1.5 are recommended; however, these values depend upon the project scale and adequacy of the input and calibrating [54,55]. A larger P-factor can be achieved at the expense of a large R-factor; hence, a balance must be reached between the two.

The SWAT-CUPP program was used for calibration. The model performance was defined based on the Nash–Sutcliffe model efficiency coefficient (NSE), the coefficient of determination (R^2), percent bias (PBIAS), and RMSE-observations standard deviation ratio (RSR) [55,57]. NSE values can range between $-\infty$ to 1, which measures how well the simulated output matches the observed data along a 1:1 line (regression line with slope equal to 1). The NSE value greater than 0.5 for a monthly time step is applicable to the catchment and the impact analysis [53,57]. R^2 statistics can range from 0 to 1, where 0 indicates no correlation and 1 indicates perfect correlation. R^2 value greater than 0.5 is considered acceptable [58,59].

The calibration period for this study was 1990–1998, which means measured observed data of this time period were used with different adjusted parameter value ranges to fit with the simulated model. After calibration was obtained, the model was validated with calibrated parameter ranges using observed data from 1999–2005. Discharge was calibrated at first, as it is the primary controlling variable [50]. Similar processes were repeated for the sediment load obtained from the LOADEST model.

The output from the SWAT model was simulated using the land cover data for the year 2001. The result was then used for model calibration and validation. Land cover data for the year 2016 and weather data from the year 2005 to 2016 were used to observe the relationship between land cover change and discharge and sediment. DEM and soil data were kept the same when the model was a rerun. The change in discharge and sediment was compared using the simulated results obtained from the two different land cover data.

3. Results

3.1. Calibration, Uncertainty, and Validation of Discharge

Figures 6 and 7 show the graphical representation of observed and simulated discharge data during the calibration and validation period. The calibrated model attained a P-factor of 0.50. This represents that 50% of the measured discharge data was bracketed by 95PPU within the model uncertainty prediction. The P-factor during the validation period was 0.62, which is higher than calibrated. The R-factor had the desired value of 0.83 and 1.04 during calibration and validation (which are less than 1.5).

Table 4 shows statistical parameters NSE, R^2 , PBIAS, and RSR values estimated as 0.76, 0.85, 5.4, and 0.49 during calibration, and 0.74, 0.8, 12.2, and 0.51 during validation, respectively. The NSE and R^2 values were greater than 0.7 for both calibration and validation periods, suggesting a good match between measured and simulated monthly discharge data [53,57].

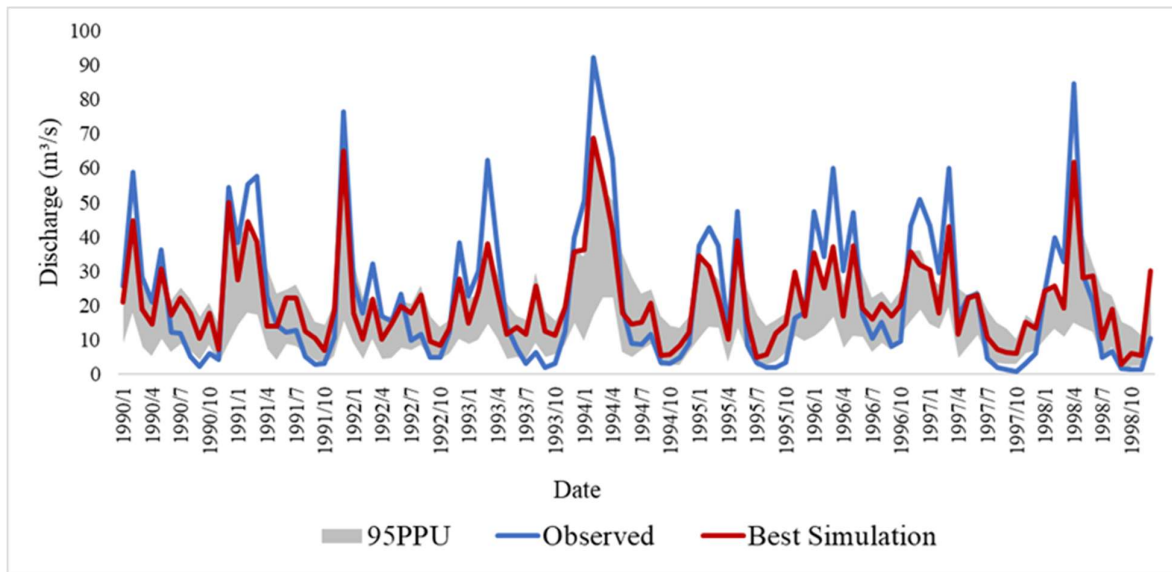


Figure 6. Observed and simulated monthly discharge data during the calibration period (1990–1998) at the Cumberland River in the watershed under study.

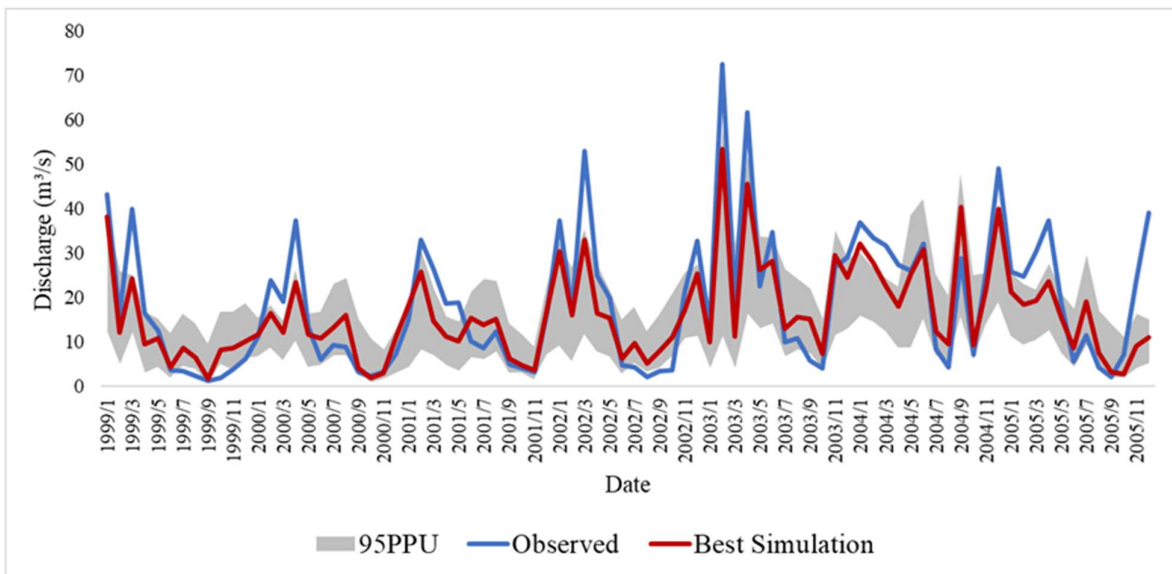


Figure 7. Observed and simulated monthly discharge data during the validation period (1999–2005) at the Cumberland River in the watershed under study.

Table 4. Statistical results of model calibration and validation accuracy for discharge.

Calibration/Validation	Criteria	Value
Calibration (1990–1998)	NSE	0.76
	R ²	0.85
	PBIAS	5.4
	RSR	0.49
	P-factor	0.5
	R-factor	0.83

Table 4. Cont.

Calibration/Validation	Criteria	Value
Validation (1999–2005)	NSE	0.74
	R ²	0.8
	PBIAS	12.2
	RSR	0.51
	P-factor	0.62
	R-factor	1.04

3.2. Calibration, Uncertainty, and Validation of Sediment

Sediment was found to be the most sensitive to $v_CH_N2.rte$ (p -value = 0, t -stat = -20.88), $r_CN2.mgt$ (p -value = 0, t -stat = 6.43), $v_ALPHA_BF.gw$ (p -value = 0.05, t -stat = 1.88). The graphical representation of monthly sediment data during the calibration and validation period is shown in Figures 7 and 8, respectively. The P-factor was 0.91 during calibration and 0.90 during validation. This represents that 95PPU bracketed 91% and 90% of observations during calibration and validation, respectively. The R-factor was 1.60 during calibration and 1.79 during validation, which represents the uncertainties of the model. P-factor and R-factor are used to judge the strength of calibration and validation [45]. Our result showed strong statistical agreement with more than 90% of observed data enveloped by our modeling result, shown as the 95PPU graph in Figures 8 and 9.

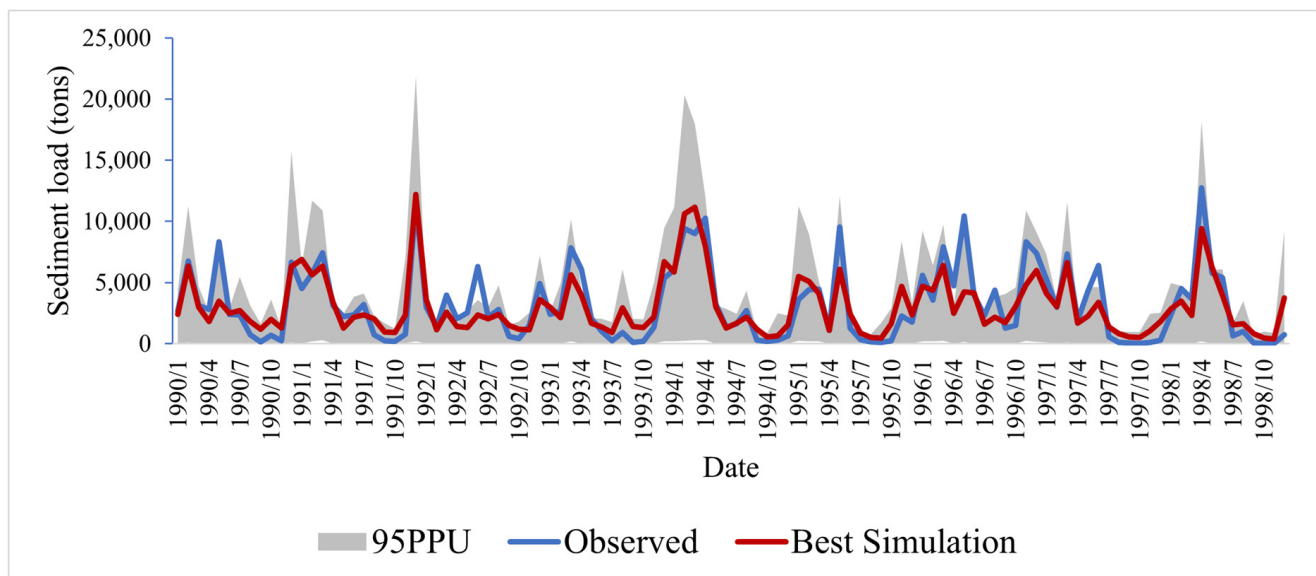


Figure 8. Observed and simulated monthly sediment during the calibration period (1990–1998) at the Cumberland River in the watershed under study.

Similarly, the R², NSE, PBIAS, and RSR values during calibration were 0.75, 0.74, 5.9, and 0.51, and during validation, were 0.68, 0.67, 2.8, and 0.57, respectively, as shown in Table 5. The model accuracy was satisfied with the desired values for NSE, R², RSR, and PBIAS according to the guidelines, which represented a close relationship between observed and simulated sediment yields [53,57]. PBIAS values were low and positive, which indicated accurate model simulation.

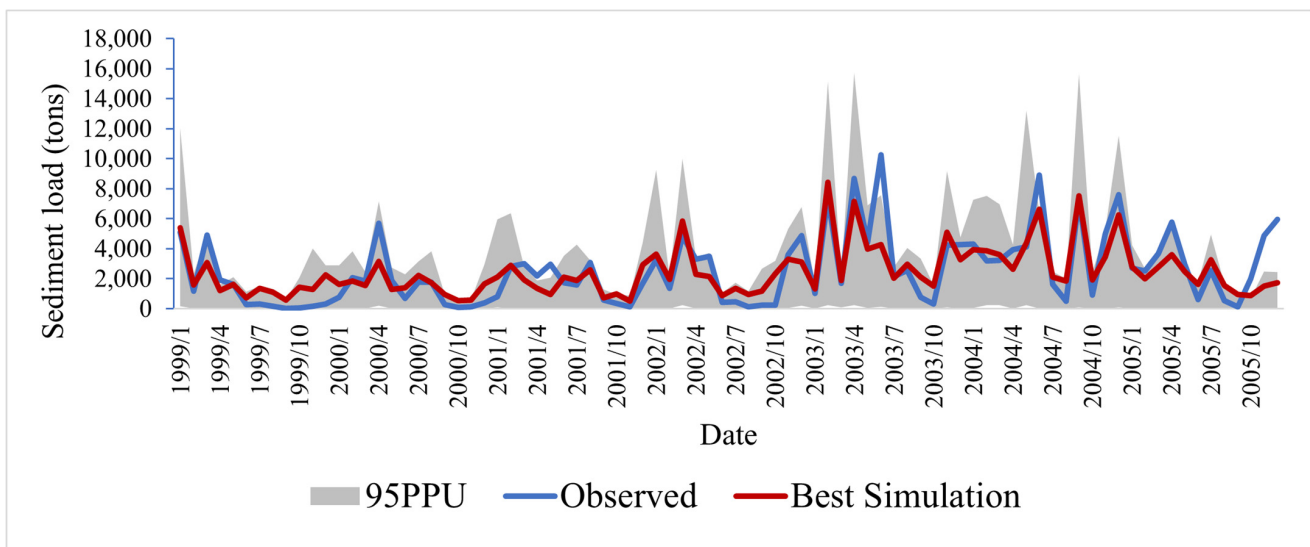


Figure 9. Observed and simulated monthly sediment during the validation period (1999–2005) at the Cumberland River in the watershed under study.

Table 5. Statistical results of model calibration and validation accuracy for sediment.

Calibration/Validation	Criteria	Value
Calibration (1990–1998)	NSE	0.74
	R ²	0.75
	PBIAS	5.9
	RSR	0.51
	P-factor	0.91
	R-factor	1.6
Validation (1999–2005)	NSE	0.67
	R ²	0.68
	PBIAS	2.8
	RSR	0.57
	P-factor	0.9
	R-factor	1.79

3.3. Land Use Land Cover Change Characteristics

Land cover classes considered in this study include water, developed, barren, forest, shrubland, and pasture/grassland, and are shown for 2001 and 2016 in Figure 10, respectively. From these figures, we can observe that previously forested areas have been converted into shrubland and pasture/grassland, which can be attributed to reclaimed mined areas.

The percentage change of different land cover classes is shown in Table 6. The watershed was overall dominated by forest, followed by developed and pasture/grassland. From the years 2001 to 2016, forest decreased by 2.4%, while developed area increased by 0.1%, barren land increased by 0.3%, shrubland increased by 0.5%, and pasture/grassland increased by 1.4%. Changes in forest areas indicate that the site was affected by human activities. With the increase in human demand to extract natural resources, forest areas decreased. Additionally, human activities such as surface mining and reclamation activities leave the land barren or convert the forest land into developed, shrubland, or pasture/grassland.

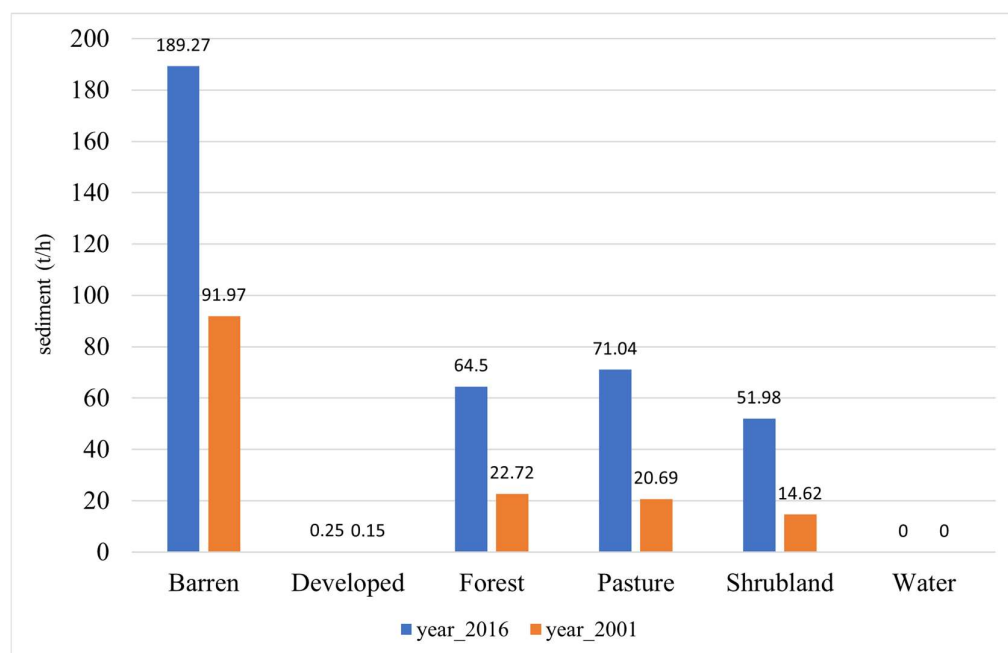


Figure 10. Contribution of different land cover classes on sediment yield between the years 2001 and 2016.

Table 6. Percentage of land cover classes and their change from 2001 to 2016.

Land Cover Class	2001	2016	% Difference
	Area (%)	Area (%)	
Water	0.2	0.2	−0.01
Developed	5.5	5.6	0.1
Barren	1.0	1.3	0.3
Forest	90.0	87.1	−2.4
Shrubland	1.0	1.6	0.5
Pasture/Grassland	2.4	3.9	1.4
Total	100	100	

The contribution of sediment yield from different land cover classes has increased from the year 2001 to 2016 (Figure 10). An increase in barren, developed pasture and shrubland leads to an increase in discharge and sediment yield, as barren and developed lands have an erosive property with no water-holding capacity, while pasture and shrubland have less water-holding capacity compared to forest land. The sediment yield from forest land also increased from 2001 to 2016. The watershed is dominated by forest, and several mining operations were in existence during the period resulting in changes in land cover. Such practices disrupted the hydrological cycle of a drainage basin and altered the sediment yield.

3.4. The Response of Discharge and Sediment under Different Land Cover Scenarios

Table 7 shows the impact of land cover changes on surface runoff and sediment yield. The result shows that annual surface runoff increased from 92.3 mm/year to 104.7 mm/year from 2001 to 2016. Similarly, annual sediment yield increased from 0.83 t/ha to 1.63 t/ha, representing a 19.35% change. Furthermore, results found that potential evapotranspiration and lateral flow increased from 595 mm to 607.4 mm, and 541.6 mm to 562.6 mm, between 2001 and 2016, respectively. The loss of water due to evapotranspiration is related to the fact that the forest is the major land cover class in this watershed. The increase in lateral flow can be attributed to soil properties and land cover class in the watershed. Increased surface runoff indicates a lower infiltration capacity of the land surface. Similarly, an increase in

sediment is due to a decrease in forest area. Barren land, followed by pastures/grassland and shrubland, additionally contributed to soil erosion and increased sediment yield.

Table 7. Estimated water balance components under two different land cover scenarios.

Component	Land Cover		
	2001	2016	%Change
Surface Runoff (mm)	92.3	104.7	11.8
Sediment Yield (t/ha)	0.8	1.63	49.0
Potential Evapotranspiration (mm)	595.5	607.4	1.9
Lateral Flow (mm)	541.6	562.6	3.7

4. Discussion

This study simulated discharge and sediment over 19 years using the SWAT model and analyzed the relationship between land cover pattern, discharge, and sediment at a monthly scale. SWAT-CUPP was used to calibrate and predict the model performance. The calibration results showed that the uncertainties indicated by 95PPU (P-factor and R-factor) shown in Table 5 for discharge are desirable. However, the observed peak values for discharge were not falling under the 95PPU band, as shown in Figures 5 and 6. A similar finding was also reported by Narsimlu et al. [60]. Several factors cause model uncertainties, such as conceptual simplifications (e.g., SCS curve number method for flow partitioning), natural and human-induced processes occurring in the watershed but not included in the program (e.g., wind erosion), occurrences of landslides, large construction (roads, bridges), and so on [55]. The increase in discharge may be due to more water being added through rainfall and tributary streams into the main channel, impervious layer, and human activities such as disturbances in the landscape. According to Zhang et al. [35], precipitation is the fundamental factor in the formation of runoff, and an increase in precipitation leads to an increase in stream discharge [35]. They also mentioned that temperature affects runoff and sediment yield, as an increase in temperature will cause an increase in evapotranspiration as well as an increase in soil moisture deficit. The lower P-factor during calibration, as compared to validation, indicates the uncertainties in input variables such as rainfall.

A study conducted by the University of Kentucky Animal Research Center in north-central Kentucky reported the SWAT model as an effective tool for simulating monthly runoff, with NSE values of 0.58 during calibration and 0.89 during validation [39]. Another study used SWAT-CUP to calibrate the model and found acceptable model performance in terms of NSE values (0.67 during calibration and 0.84 during validation) for runoff in the Chiquapin watershed of the Atlantic Coastal Plain [61]. Tang et al. [62] performed model calibration and uncertainty using SWAT-CUP and found P-factor 0.85 and 0.83, and R-factors 1.12 and 2.15, during the calibration and validation period, respectively. They further satisfied the model with NSE values of 0.77 (calibration) and 0.74 (validation) for monthly runoff. A study on a watershed in Morocco also successfully calibrated the SWAT model for monthly discharge (NSE = 0.76) and sediment (NSE = 0.69) [63]. Jha et al. [64] also used LOADEST to estimate sediment in the Upper Mississippi river basin. They simulated the model on a monthly basis and found an NSE value of 0.66 during calibration and 0.54 during validation. These results from previous studies are in accordance with our statistical results for our model performance.

Gyawali et al. [41] observed that topography dominates flow dynamics in a mountainous watershed, causing surface runoff and increasing sediment yield. Our findings are consistent with the results of this study. The SWAT model's parameter sensitivity is dependent on climate, land use, topography, and soil types, resulting in sensitivity outcomes that are specific to watersheds [65]. Therefore, a sensitivity analysis has to be carried out independently for each study area.

In this study, we investigated the overall spatial distribution pattern of land cover change (between 2001 and 2016) with annual discharge and sediment yield in the Cumberland River near Harlan watershed, Kentucky. We found that the forest area decreased,

whereas pasture, shrubland, and developed areas increased from the year 2001 to 2016 (Table 6). In addition, results showed that the surface runoff and sediment increased by 11.8% and 47.07% from the year 2001 to 2016, respectively. This implies that land cover change, i.e., conversion of forest area into other land cover types (including pasture/grassland, shrubland, barren land), has an impact on the annual water balance in the watershed. Changes in runoff and sediment yield could be justified due to changes in forest land as well as sediment transport from mining fields, pasture/grassland, and built-up areas [3,24]. Several studies have suggested that hydrology changes in response to land cover change. A study conducted by Ngo et al. [66] found an increase in annual surface runoff from 182.5 mm to 342.7 mm due to drastic changes in forest land into other land cover types between the years 1995 and 2005. Pokhrel [33] also found an increase in runoff from 171.99 mm/year to 219.17 mm/year, an increase in sediment from 2.99 mt/ha to 3.15 mt/ha with a decrease in the forest, and an increase in built-up areas from 2000 to 2010 in Khokana Outlet of the Bagmati River, Nepal. Similarly, several other studies reported the effect of historical land cover change on runoff and sediment [37,67,68]. Their results are consistent with the results of our study.

5. Conclusions

In this research, a GIS-based hydrological tool, the SWAT model, was used to simulate discharge and sediment under two different land cover scenarios to quantify the response of hydrological characteristics to land cover change. The SWAT model was successfully applied to estimate the discharge and sediment yield. SWAT-CUPP was used to perform the sensitivity analysis, calibration, uncertainty analysis, and validation of the model. Using the recommended statistical parameters (NSE, R^2 , RSR, and PBIAS), model performance was evaluated, which showed that the estimated discharge and sediment at the outlet obtained from the SWAT model indicated good agreement with the observed data.

The land cover data reveals that the watershed is dominated by forest, followed by pasture/grassland, shrubland, and barren land. From the years 2001 to 2016, changes in the land cover types of the watershed showed a decrease in forest area and an expansion of the pasture/grassland. Such change was attributed to the destruction of forest land for surface mining purposes, then reclamation of previously surface-mined areas through their conversion to grassland. The relationship of land cover change with annual discharge and sediment was also determined. The discharge and sediment yield were found to be relatively higher from the land cover data of 2016 as compared to the year 2001, which implies that land cover changes, specifically ongoing mining activities and increasing pasture/grassland, have contributed to increased surface runoff and sediment yield in the watershed. Therefore, a viable and realistic strategy is needed for the sustainable management of water resources in the watershed. Best management practices (BMPs), such as the protection of forests and the use of vegetative riparian buffers, could be applied to control the sediment transport in the river channel.

The SWAT model was efficient and effective in quantifying the discharge and sediment yield response to land cover change; however, there were some limitations in this study. During the data acquisition period of this research, it was found that regular monitoring of sediment data was not conducted. This research suggests conducting water quality monitoring programs at major river outlet basins for a systematic study of watersheds in Kentucky. Even though there exist some limitations and uncertainties in SWAT, a well-calibrated SWAT model can simulate discharge and sediment related to the land cover change. This study provides valuable information for land managers about the effect of land cover change on soil and water conservation in the Cumberland River near Harlan, which has experienced surface mining and reclamation activities. Further study on the influence of anthropogenic causes of land use change on discharge and sediment yield, as well as possible climate change impacts at river basins, is recommended.

Author Contributions: S.K.: Conceptualization, Methodology, Formal Analysis, Writing—original draft. B.G.: Conceptualization, Funding acquisition, Software, Writing—review and editing. S.S.: Conceptualization, Methodology, Writing—review and editing. D.Z.: Writing—review and editing. George Antonious: Writing—review and editing. M.G.: Writing—review and editing. B.P.: Writing—review and editing. All authors have read and agreed to the published version of the manuscript.

Funding: This research was supported by (1) USDA/NIFA Evans Allen Fund (Project # KYX-10-17-59P, Accession # 1014433; 2018-2021) (2) USDA/AFRI (Award #2019-68006-29330, 2019-2021). Gyawali's 20% of time on this paper was supported by NSF-HBCU-UP (Award # HRD 1912413 2019-2021; and NSF-HBCU-UP (Award # HRD 2011917).

Data Availability Statement: Not applicable.

Acknowledgments: The authors are thankful to the unanimous reviewers, editors, and the media and communication editor in the College of Agriculture, Community, and the Sciences at Kentucky State University.

Conflicts of Interest: The authors declare no conflict of interest. The funders had no role in the design of the study; in the collection, analyses, or interpretation of data; in the writing of the manuscript; or in the decision to publish the results.

Patents: There are no patents resulting from the work reported in this manuscript.

Declaration of Competing Interest: The authors declare that they have no known competing financial interests or personal relationships that could have appeared to influence the work reported in this paper.

Appendix A. SSURGO Soil Class Descriptions

Mapunit Symbol	Mapunit Name
17F	Gilpin–Berks complex, 55 to 70 percent slopes
29F	Gilpin–Summers–Kimper complex, 20 to 55 percent slopes, very stony
35F	Wallen–Rock outcrop complex, 35 to 85 percent slopes, very stony
6E	Bethesda, Fairpoint, and Sewell soils, 0 to 80 percent slopes, very rocky
AgB	Allegheny loam, 2 to 6 percent slopes
A1C	Allegheny loam, 2 to 15 percent slopes
AtF	Alticrest–Ramsey–Wallen complex, 20 to 55 percent slopes, rocky
Bo	Bonnie silt loam, occasionally flooded
CgF	Cloverlick–Guyandotte–Highsplint complex, 20 to 80 percent slopes, very stony
CkF	Cloverlick–Kimper–Highsplint complex, 30 to 65 percent slopes, very stony
Cr	Craigsville–Philo complex, occasionally flooded
DrF	Dekalb–Gilpin–Rayne complex, 25 to 65 percent slopes, very rocky
Du	Dumps, Mine; tailings; and Tipples
FbC	Fairpoint and Bethesda soils, 2 to 20 percent slopes
FbF	Fairpoint and Bethesda soils, 20 to 70 percent slopes, stony
FkE	Fiveblock and Kaymine soils, 0 to 30 percent slopes, stony
GI D	Gilpin–Shelocta complex, 12 to 25 percent slopes
GmF	Gilpin–Summers–Kimper complex, 20 to 55 percent slopes, very stony
GsC	Gilpin–Shelocta silt loams, 3 to 12 percent slopes
GsD	Gilpin–Shelocta silt loams, 12 to 20 percent slopes
GtF	Gilpin–Rayne–Sequoia complex, 25 to 55 percent slopes, very stony
HeF	Helechawa–Varilla–Jefferson complex, 35 to 75 percent slopes, very rocky
HgD	Highsplint very flaggy silt loam, 5 to 20 percent slopes, extremely bouldery
HsF	Highsplint–Shelocta–Dekalb complex, 35 to 80 percent slopes, very stony
Hy	Holly loam, frequently flooded
JfD	Jefferson gravelly silt loam, 12 to 20 percent slopes

Mapunit Symbol	Mapunit Name
KfF	Kaymine, Fairpoint, and Fiveblock soils, benched, 2 to 70 percent slopes, very stony
KmD	Kimper silt loam, 5 to 20 percent slopes, very stony
KrF	Kimper–Cloverlick–Renox complex, 30 to 80 percent slopes, extremely stony
Ph	Philo fine sandy loam, occasionally flooded
Po	Pope fine sandy loam, occasionally flooded
SeB	Shelocta gravelly silt loam, 2 to 6 percent slopes
SeC	Shelocta channery silt loam, 6 to 12 percent slopes
SgE	Shelocta–Gilpin silt loams, 20 to 35 percent slopes
ShF	Shelocta–Highsplint–Gilpin complex, 20 to 70 percent slopes, very stony
SkF	Shelocta–Kimper–Cloverlick complex, 20 to 80 percent slopes, very stony
SmF	Shelocta–Kimper–Cutshin complex, 20 to 55 percent slopes, very stony
Ud	Udorthents–Urban land complex, occasionally flooded
uDut	Dumps, mine, and tailings
uGrig	Grigsby fine sandy loam, 0 to 3 percent slopes, frequently flooded
uMgmF	Matewan–Gilpin–Marrowbone complex, 12 to 80 percent slopes, very rocky
UrC	Udorthents–Urban land complex, 3 to 15 percent slopes
UrE	Udorthents–Urban land complex, 15 to 35 percent slopes
uRgrB	Rowdy–Grigsby complex, 0 to 6 percent slopes, occasionally flooded
uShgF	Shelocta–Highsplint–Gilpin complex, 20 to 70 percent slopes, very stony
uUdoC	Udorthents–Urban land complex, 0 to 15 percent slopes
uUdrB	Udorthents–Urban land–Grigsby complex, 0 to 6 percent slopes, occasionally flooded
uUduE	Udorthents–Urban land–Rock outcrop complex, 0 to 35 percent slopes
VaF	Varilla–Jefferson–Alticrest complex, 35 to 75 percent slopes, very rocky
VrD	Varilla very stony loam, 5 to 20 percent slopes, extremely bouldery

References

- NOAA. What Is a Watershed? 2020. Available online: <https://oceanservice.noaa.gov/facts/watershed.html> (accessed on 9 February 2020).
- NOAA. What Is the Difference between Land Cover and Land Use? 2021. Available online: <https://oceanservice.noaa.gov/facts/lclu.html> (accessed on 19 February 2021).
- Khoi, D.N.; Suetsugi, T. The responses of hydrological processes and sediment yield to land-use and climate change in the Be River Catchment, Vietnam. *Hydrol. Process.* **2014**, *28*, 640–652. [\[CrossRef\]](#)
- Bian, G.; Zhang, J.; Chen, J.; Wang, G.; Song, M. Spatial and seasonal variations of hydrological responses to climate and land-use changes in a highly urbanized basin of Southeastern China. *Hydrol. Res.* **2021**, *52*, 506–522. [\[CrossRef\]](#)
- Getachew, B.; Manjunatha, B.; Bhat, H.G. Modeling projected impacts of climate and land use/land cover changes on hydrological responses in the Lake Tana Basin, upper Blue Nile River Basin, Ethiopia. *J. Hydrol.* **2021**, *595*, 125974. [\[CrossRef\]](#)
- Aredo, M.R.; Hatiye, S.D.; Pingale, S.M. Impact of land use/land cover change on stream flow in the Shaya catchment of Ethiopia using the MIKE SHE model. *Arab. J. Geosci.* **2021**, *14*, 1–15. [\[CrossRef\]](#)
- Li, Z.; Liu, W.; Zhang, J.; Zheng, F.-L. Impacts of land use change and climate variability on hydrology in an agricultural catchment on the Loess Plateau of China. *J. Hydrol.* **2009**, *377*, 35–42. [\[CrossRef\]](#)
- Buendia, C.; Bussi, G.; Tuset, J.; Vericat, D.; Sabater, S.; Palau, A.; Batalla, R. Effects of afforestation on runoff and sediment load in an upland Mediterranean catchment. *Sci. Total Environ.* **2016**, *540*, 144–157. [\[CrossRef\]](#)
- Birkinshaw, S.J.; Guerreiro, S.B.; Nicholson, A.; Liang, Q.; Quinn, P.; Zhang, L.; He, B.; Yin, J.; Fowler, H.J. Climate change impacts on Yangtze River discharge at the Three Gorges Dam. *Hydrol. Earth Syst. Sci.* **2017**, *21*, 1911–1927. [\[CrossRef\]](#)
- Yonaba, R.; Biaou, A.C.; Koïta, M.; Tazen, F.; Mounirou, L.A.; Zouré, C.O.; Quelo, P.; Karambiri, H.; Yacouba, H. A dynamic land use/land cover input helps in picturing the Sahelian paradox: Assessing variability and attribution of changes in surface runoff in a Sahelian watershed. *Sci. Total Environ.* **2020**, *757*, 143792. [\[CrossRef\]](#)
- Turner, B.L., II; Lambin, E.F.; Reenberg, A. The emergence of land change science for global environmental change and sustainability. *Proc. Natl. Acad. Sci. USA* **2007**, *104*, 20666–20671. [\[CrossRef\]](#)
- Mi, J.; Yang, Y.; Zhang, S.; An, S.; Hou, H.; Hua, Y.; Chen, F. Tracking the Land Use/Land Cover Change in an Area with Underground Mining and Reforestation via Continuous Landsat Classification. *Remote Sens.* **2019**, *11*, 1719. [\[CrossRef\]](#)
- Höök, M.; Aleklett, K. Historical trends in American coal production and a possible future outlook. *Int. J. Coal Geol.* **2009**, *78*, 201–216. [\[CrossRef\]](#)
- Turner, M.G.; Ruscher, C.L. Changes in landscape patterns in Georgia, USA. *Landscape Ecol.* **1988**, *1*, 241–251. [\[CrossRef\]](#)

15. USEPA. *The Effects of Mountaintop Mines and Valley Fills on Aquatic Ecosystems of the Central Appalachian Coalfields*; EPA/600/R-09/138F; USEPA: Washington, DC, USA, 2011. Available online: <https://cfpub.epa.gov/ncea/risk/recordisplay.cfm?deid=225743> (accessed on 17 March 2020).
16. Bajocco, S.; De Angelis, A.; Perini, L.; Ferrara, A.; Salvati, L. The Impact of Land Use/Land Cover Changes on Land Degradation Dynamics: A Mediterranean Case Study. *Environ. Manag.* **2012**, *49*, 980–989. [[CrossRef](#)] [[PubMed](#)]
17. Tadesse, L.; Suryabhadgavan, K.; Sridhar, G.; Legesse, G. Land use and land cover changes and Soil erosion in Yezat Watershed, North Western Ethiopia. *Int. Soil Water Conserv. Res.* **2017**, *5*, 85–94. [[CrossRef](#)]
18. Hooke, R.L. Spatial distribution of human geomorphic activity in the United States: Comparison with rivers. *Earth Surf. Process. Landforms* **1999**, *24*, 687–692. [[CrossRef](#)]
19. Huang, Y.; Tian, F.; Wang, Y.; Wang, M.; Hu, Z. Effect of coal mining on vegetation disturbance and associated carbon loss. *Environ. Earth Sci.* **2014**, *73*, 2329–2342. [[CrossRef](#)]
20. Ross, M.R.V.; McGlynn, B.L.; Bernhardt, E.S. Deep Impact: Effects of Mountaintop Mining on Surface Topography, Bedrock Structure, and Downstream Waters. *Environ. Sci. Technol.* **2016**, *50*, 2064–2074. [[CrossRef](#)]
21. California Department of Conservation. 2019. Available online: <https://www.conservation.ca.gov/dmr/SMARA%20Mines/reclamation> (accessed on 17 March 2018).
22. Wang, C.; Lv, Y.; Song, Y. Researches on mining subsidence disaster management GIS's system. In Proceedings of the 2012 International Conference on Systems and Informatics (ICSAI2012), Yantai, China, 19–20 May 2012; pp. 2493–2496. [[CrossRef](#)]
23. Eastern Kentucky Coalfield. *Wikipedia*. 2021. Available online: https://en.wikipedia.org/wiki/Eastern_Kentucky_Coalfield (accessed on 15 January 2021).
24. Gurung, K.; Yang, J.; Fang, L. Assessing Ecosystem Services from the Forestry-Based Reclamation of Surface Mined Areas in the North Fork of the Kentucky River Watershed. *Forests* **2018**, *9*, 652. [[CrossRef](#)]
25. Bai, Y.; Ochuodho, T.O.; Yang, J. Impact of land use and climate change on water-related ecosystem services in Kentucky, USA. *Ecol. Indic.* **2019**, *102*, 51–64. [[CrossRef](#)]
26. Kentucky Division of Water. Kentucky Nonpoint Source Management Plan: A Strategy for 2019–2023. 2019. Available online: https://services.statescape.com/ssu/Regs/ss_8586430572245812376.pdf (accessed on 15 January 2021).
27. Kentucky Geological Survey. Water Fact Sheet. 2021. Available online: <https://www.uky.edu/KGS/water/> (accessed on 9 February 2020).
28. Phillips, J.D. Impacts of surface mine valley fills on headwater floods in eastern Kentucky. *Environ. Earth Sci.* **2004**, *45*, 367–380. [[CrossRef](#)]
29. Negley, T.L.; Eshleman, K.N. Comparison of stormflow responses of surface-mined and forested watersheds in the Appalachian Mountains, USA. *Hydrol. Process.* **2006**, *20*, 3467–3483. [[CrossRef](#)]
30. Evans, D.M.; Zipper, C.E.; Hester, E.T.; Schoenholtz, S.H. Hydrologic effects of surface coal mining in Appalachia (US). *J. Am. Water Resour. Assoc.* **2015**, *51*, 1436–1452. [[CrossRef](#)]
31. Clark, E.V.; Zipper, C.E.; Soucek, D.J.; Daniels, W.L. Contaminants in Appalachian water resources generated by non-acid-forming coal-mining materials. In *Appalachia's Coal Mined Landscapes*; Chapter 9; Zipper, C.E., Skousen, J.G., Eds.; Springer: Berlin/Heidelberg, Germany, 2021.
32. Arnold, J.G.; Srinivasan, R.; Muttiah, R.S.; Williams, J.R. Large area hydrologic modeling and assessment part I: Model development 1. *J. Am. Water Resour. Assoc.* **1998**, *34*, 73–89. [[CrossRef](#)]
33. Pokhrel, B.K. Impact of Land Use Change on Flow and Sediment Yields in the Khokana Outlet of the Bagmati River, Kathmandu, Nepal. *Hydrology* **2018**, *5*, 22. [[CrossRef](#)]
34. Shang, X.; Jiang, X.; Jia, R.; Wei, C. Land Use and Climate Change Effects on Surface Runoff Variations in the Upper Heihe River Basin. *Water* **2019**, *11*, 344. [[CrossRef](#)]
35. Zhang, S.; Li, Z.; Hou, X.; Yi, Y. Impacts on watershed-scale runoff and sediment yield resulting from synergetic changes in climate and vegetation. *CATENA* **2019**, *179*, 129–138. [[CrossRef](#)]
36. Kateb, Z.; Bouchelkia, H.; Benmansour, A.; Belarbi, F. Sediment transport modeling by the SWAT model using two scenarios in the watershed of Beni Haroun dam in Algeria. *Arab. J. Geosci.* **2020**, *13*, 1–17. [[CrossRef](#)]
37. Sinha, R.K.; Eldho, T.I.; Subimal, G. Assessing the impacts of land cover and climate on runoff and sediment yield of a river basin. *Hydrol. Sci. J.* **2020**, *65*, 2097–2115. [[CrossRef](#)]
38. Aboelnour, M.; Gitau, M.W.; Engel, B.A. Hydrologic Response in an Urban Watershed as Affected by Climate and Land-Use Change. *Water* **2019**, *11*, 1603. [[CrossRef](#)]
39. Spruill, C.A.; Workman, S.R.; Taraba, J.L. Simulation of daily stream discharge from small watersheds using the SWAT model. *Am. Soc. Agric. Biol. Eng.* **2000**, *1*, 1431–1439. [[CrossRef](#)]
40. SWAT Literature Database. Available online: https://www.card.iastate.edu/swat_articles/ (accessed on 15 May 2021).
41. Gyawali, B.; Shrestha, S.; Bhatta, A.; Pokhrel, B.; Cristan, R.; Antonious, G.; Banerjee, S.; Paudel, K.P. Assessing the Effect of Land-Use and Land-Cover Changes on Discharge and Sediment Yield in a Rural Coal-Mine Dominated Watershed in Kentucky, USA. *Water* **2022**, *14*, 516. [[CrossRef](#)]
42. U.S. Census Bureau. QuickFacts Harlan County, Kentucky. 2020. Available online: <https://www.census.gov/quickfacts/harlandcountykentucky> (accessed on 17 March 2020).

43. Srinivasan, R.; Arnold, J.G. Integration of A Basin-Scale Water Quality Model With Gis. *JAWRA J. Am. Water Resour. Assoc.* **1994**, *30*, 453–462. [[CrossRef](#)]
44. Arnold, J.G.; Moriasi, D.N.; Gassman, P.W.; Abbaspour, K.C.; White, M.J.; Srinivasan, R.; Santhi, C.; Harmel, R.D.; van Griensven, A.; Van Liew, M.W.; et al. SWAT: Model Use, Calibration, and Validation. *Trans. ASABE* **2012**, *55*, 1491–1508. [[CrossRef](#)]
45. Zhang, P.; Liu, R.; Bao, Y.; Wang, J.; Yu, W.; Shen, Z. Uncertainty of SWAT model at different DEM resolutions in a large mountainous watershed. *Water Res.* **2014**, *53*, 132–144. [[CrossRef](#)] [[PubMed](#)]
46. Zhang, Y.; Su, F.; Hao, Z.; Xu, C.; Yu, Z.; Wang, L.; Tong, K. Impact of projected climate change on the hydrology in the headwaters of the Yellow River basin. *Hydrol. Process.* **2015**, *29*, 4379–4397. [[CrossRef](#)]
47. Neitsch, S.L.; Arnold, J.G.; Kiniry, J.R.; Williams, J.R. *Soil and Water Assessment Tool Theoretical Documentation Version 2009*; Texas Water Resources Institute: College Station, TX, USA, 2011.
48. Williams, J.R.; Berndt, H.D. Sediment Yield Prediction Based on Watershed Hydrology. *Trans. ASAE* **1977**, *20*, 1100–1104. [[CrossRef](#)]
49. Runkel, R.L.; Crawford, C.G.; Cohn, T.A. Load estimator (LOADEST): A FORTRAN program for estimating constituent loads in streams and rivers. In *USGS Techniques and Methods*; USGS Numbered Series No. 4-A5; USGS: Reston, VA, USA, 2004.
50. Abbaspour, K.C. SWAT-CUP Premium 2020: SWAT Calibration and Uncertainty Programs (Premium Versions): A User Manual. 2020. Available online: https://swat.tamu.edu/media/114860/usermanual_swatcup.pdf (accessed on 23 October 2020).
51. Servat, E.; Dezetter, A. Selection of calibration objective functions in the context of rainfall-runoff modelling in a Sudanese savannah area. *Hydrol. Sci. J.* **1991**, *36*, 307–330. [[CrossRef](#)]
52. Sao, D.; Kato, T.; Tu, L.H.; Thouk, P.; Fitriyah, A.; Oeurng, C. Evaluation of Different Objective Functions Used in the SUFI-2 Calibration Process of SWAT-CUP on Water Balance Analysis: A Case Study of the Pursat River Basin, Cambodia. *Water* **2020**, *12*, 2901. [[CrossRef](#)]
53. Moriasi, D.N.; Gitau, M.W.; Pai, N.; Daggupati, P. Hydrologic and Water Quality Models: Performance Measures and Evaluation Criteria. *Trans. ASABE* **2015**, *58*, 1763–1785. [[CrossRef](#)]
54. Abbaspour, K.C.; Yang, J.; Maximov, I.; Siber, R.; Bogner, K.; Mieleitner, J.; Zobrist, J.; Srinivasan, R. Modelling hydrology and water quality in the pre-alpine/alpine Thur watershed using SWAT. *J. Hydrol.* **2007**, *333*, 413–430. [[CrossRef](#)]
55. Abbaspour, K.C.; Rouholahnejad, E.; Vaghefi, S.; Srinivasan, R.; Yang, H.; Kløve, B. A continental-scale hydrology and water quality model for Europe: Calibration and uncertainty of a high-resolution large-scale SWAT model. *J. Hydrol.* **2015**, *524*, 733–752. [[CrossRef](#)]
56. Abbaspour, K.C.; Vaghefi, S.A.; Srinivasan, R. A Guideline for Successful Calibration and Uncertainty Analysis for Soil and Water Assessment: A Review of Papers from the 2016 International SWAT Conference. *Water* **2017**, *10*, 6. [[CrossRef](#)]
57. Moriasi, D.N.; Arnold, J.G.; van Liew, M.W.; Bingner, R.L.; Harmel, R.D.; Veith, T.L. Model evaluation guidelines for systematic quantification of accuracy in watershed simulations. *Trans. ASABE* **2007**, *50*, 885–900. [[CrossRef](#)]
58. Santhi, C.; Arnold, J.G.; Williams, J.R.; Dugas, W.A.; Srinivasan, R.; Hauck, L.M. Validation of the Swat Model on A Large Rwer Basin with Point and Nonpoint Sources. *J. Am. Water Resour. Assoc.* **2001**, *37*, 1169–1188. [[CrossRef](#)]
59. Van Liew, M.W.; Arnold, J.G.; Garbrecht, J.D. Hydrologic Simulation on Agricultural Watersheds: Choosing between Two Models. *Trans. ASAE* **2003**, *46*, 1539–1551. [[CrossRef](#)]
60. Narsimlu, B.; Gosain, A.K.; Chahar, B.R.; Singh, S.K.; Srivastava, P.K. SWAT Model Calibration and Uncertainty Analysis for Streamflow Prediction in the Kunwari River Basin, India, Using Sequential Uncertainty Fitting. *Environ. Process.* **2015**, *2*, 79–95. [[CrossRef](#)]
61. Mapes, K.L.; Pricope, N.G. Evaluating SWAT Model Performance for Runoff, Percolation, and Sediment Loss Estimation in Low-Gradient Watersheds of the Atlantic Coastal Plain. *Hydrology* **2020**, *7*, 21. [[CrossRef](#)]
62. Tang, F.; Xu, H.; Xu, Z. Model calibration and uncertainty analysis for runoff in the Chao River Basin using sequential uncertainty fitting. *Procedia Environ. Sci.* **2012**, *13*, 1760–1770. [[CrossRef](#)]
63. Briak, H.; Moussadek, R.; Aboumaria, K.; Mrabet, R. Assessing sediment yield in Kalaya gauged watershed (Northern Morocco) using GIS and SWAT model. *Int. Soil Water Conserv. Res.* **2016**, *4*, 177–185. [[CrossRef](#)]
64. Jha, M.; Gassman, P.W.; Secchi, S.; Arnold, J. Upper Mississippi River Basin modeling system part 2: Baseline simulation results. In *Coastal Hydrology and Processes*; Water Resources Publications: Highland Ranch, CO, USA, 2006.
65. Schmalz, B.; Fohrer, N. Comparing model sensitivities of different landscapes using the ecohydrological SWAT model. *Adv. Geosci.* **2009**, *21*, 91–98. [[CrossRef](#)]
66. Ngo, T.S.; Nguyen, D.B.; Rajendra, P.S. Effect of land use change on runoff and sediment yield in Da River Basin of Hoa Binh province, Northwest Vietnam. *J. Mt. Sci.* **2015**, *12*, 1051–1064. [[CrossRef](#)]
67. Zhu, C. Land Use/Land Cover Change and Its Hydrological Impacts from 1984 to 2010 in the Little River Watershed, Tennessee. *Int. Soil Water Conserv. Res.* **2014**, *2*, 11–21. [[CrossRef](#)]
68. Hovenga, P.A.; Wang, D.; Medeiros, S.C.; Hagen, S.C.; Alizad, K. The response of runoff and sediment loading in the Apalachicola River, Florida to climate and land use land cover change. *Earth's Futur.* **2016**, *4*, 124–142. [[CrossRef](#)]

Disclaimer/Publisher's Note: The statements, opinions and data contained in all publications are solely those of the individual author(s) and contributor(s) and not of MDPI and/or the editor(s). MDPI and/or the editor(s) disclaim responsibility for any injury to people or property resulting from any ideas, methods, instructions or products referred to in the content.